Municipal solid waste biochar-bentonite composite for the removal of antibiotic ciprofloxacin from aqueous media

Ahmed Ashiq[1], Nadeesh M. Adassooriya[1], Binoy Sarkar[2,3*], Anushka Upamali Rajapaksha[1], Yong Sik Ok[4], Meththika Vithanage[1, 5*]

[1] Ecosphere Resilience Research Centre, Faculty of Applied Science, University of Sri Jayewardenepura, Sri Lanka

[2] Department of Animal and Plant Sciences, The University of Sheffield, Sheffield, S10 2TN, United Kingdom

[3] Future Industries Institute, University of South Australia, Mawson Lakes, SA 5095, Australia

[4] Korea Biochar Research Center, O-Jeong Eco-Resilience Institute (OJERI) & Division of Environmental Science and Ecological Engineering, Korea University, Seoul 02841, South Korea

[5] Molecular Microbiology and Human Diseases, National Institute of Fundamental Studies, Kandy 20000, Sri Lanka

*Co-corresponding authors:

Dr Binoy Sarkar; The University of Sheffield; E-mail: b.sarkar@sheffield.ac.uk; and

Dr Meththika Vithanage; University of Sri Jayewardenepura; E-mail: meththika@sjp.ac.lk

Highlights

- Clay-biochar composite was prepared using municipal solid waste and bentonite
- The composite adsorbed ciprofloxacin more efficiently than pristine materials
- The antibiotic may have intercalated in the clay interlayers of the composite
- Cooperative adsorption mechanism was suggested by data modeling

Graphical abstract

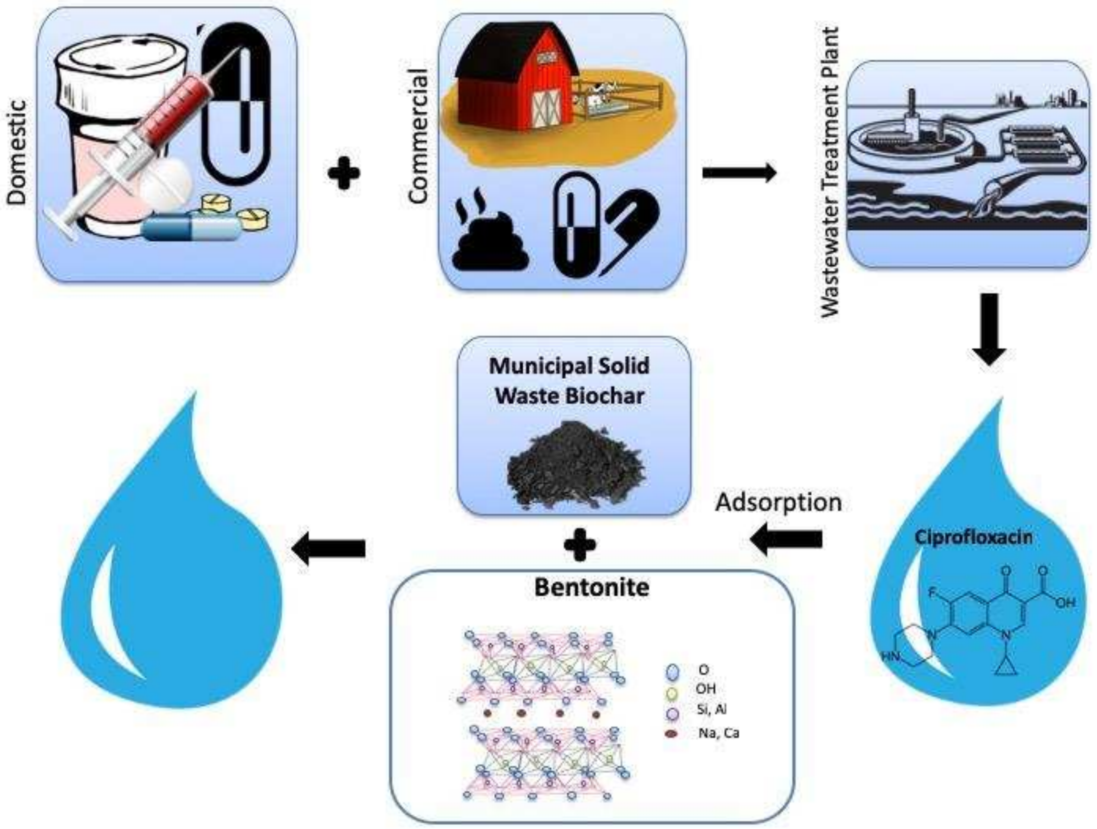

Abstract

This study investigates the adsorption of ciprofloxacin (CPX) onto a municipal solid waste derived biochar (MSW-BC) and a composite material developed by combining the biochar with bentonite clay. A bentonite-MSW slurry was first prepared at 1:5 ratio (w/w), and then pyrolyzed at 450°C for 30 min. The composite was characterized by scanning electron microscopy (SEM), Powder X-ray diffraction (PXRD) and Fourier transform infrared (FTIR) spectroscopy before and after CPX adsorption. Batch experiments were conducted to assess the effect of pH, reaction time and adsorbate dosage. The SEM images confirmed successful modification of the biochar with bentonite showing plate like structures. The PXRD patterns showed changes in the crystalline lattice of both MSW-BC and the composite before and after CPX adsorption whereas the FTIR spectra indicated merging and widening of specific bands after CPX adsorption. The optimum CPX adsorption was achieved at pH 6, and the maximum adsorption capacity of the composite calculated via isotherm modeling was 190 mg/g, which was about 40% higher than the pristine MSW-BC. The Hill isotherm model along with pseudo-second order and Elovich kinetic models showed the best fit to the adsorption data. The most plausible mechanism for increased adsorption capacity is the increased active sites of the composites for CPX adsorption through induced electrostatic interactions between the functional groups of the composites and CPX molecule. The added reactive surfaces in the composite because of bentonite incorporation, and the intercalation of CPX in the clay interlayers improved the adsorption of CPX by the biochar-bentonite composite compared to the pristine biochar. Thus, MSW-BC-bentonite composites could be considered as a potential material for remediating pharmaceuticals in aqueous media.

Keywords: Water treatment; Engineered biochar; Emerging contaminants; Antibiotics; Clay composites

1. Introduction

In the recent past, antibiotics have emerged as an important group of environmental pollutants that is extremely challenging to remediate in the water systems (Kanakaraju et al., 2018; Philip et al., 2018). Extensive usage of antibiotics in human and veterinary medicines have revolutionized treatment of diseases, and are mostly used as inhibitors and biocides of pathogenic microorganisms. They have also been used as growth promoters in the animal feed industry, especially in aquaculture, poultry, beekeeping, and livestock (Sarmah et al., 2006). Despite antibiotics designed to treat ailments of humans and animals, their continuous presence in the groundwater, urban wastewater and drinking water has become a threat to the environmental quality. Thus, these organic pollutants have been considered as contaminants of emerging concern since the last two decades (Kanakaraju et al., 2018; Oberlé et al., 2012; Sanderson et al., 2016). They have been listed as priority risk group of contaminants due to their toxicity to algae and bacteria even at nanogram level of concentration creating a disturbance in the natural ecosystems (Huang et al., 2017; Philip et al., 2018; Yi et al., 2017).

Antibiotics such as norfloxacin, sulfamethoxazole, tetracyclines, sulphonamides, macrolides and quinolones have been detected alarmingly in wastewater effluents, river water and ground water in various parts of the world (Azanu et al. 2018; Kim et al. 2015; Yi et al. 2017). Extensive studies are being carried out for tetracycline, sulfamethazine and sulfonamide based antibiotics in the aqueous media, but studies on ciprofloxacin (CPX), which is a quinolone compound, are limited despite its extensive use in humans and veterinary animals. Few previous studies indicated CPX concentrations in the range of 0.01-0.03 mg/L in wastewater streams (Maul et al., 2006), 0.75 mg/kg in animal feeds (Martínez-Carballo et al., 2007), and 0.64-45.59 mg/kg in animal excreta (Li et al., 2018; Zhao et al., 2010). Larsson et al. (2007) confirmed the presence of 31 mg/L of CPX in wastewater from industrial effluent. Approximately, 40-60% of CPX administered to humans get excreted as such increasing the toxicity in the natural systems (Espinosa et al., 2015; Li et al., 2014; Patrolecco et al., 2018). The degradation pathways of CPX remains a question of debate as it does not get easily degraded except with a particular kind of bacteria (Labrys poetucalensis) (Amorim et al., 2014). Liao et al. (2016) suggested that with the increase in temperature, the CPX degradation rapidly increases and the supplement of glucose or nitrogen could improve the degradation rate. However, such scenarios do not sound feasible in the open environmental conditions. The high environmental occurrence level of CPX together with its persistence nature and potential to form antibiotic resistance like other antibiotic compounds urge to remediate CPX in soils and aquatic bodies.

Conventional water treatment systems do not mitigate CPX (Azanu et al. 2018; Li and Zhang 2010), and as a result, adsorption method is widely used due to the ease of operation and cheap costs (Yu et al., 2016). For choosing the adsorbents, well-developed porous structures, large surface area, modification of surface functional groups and cheap and easy availability of the materials are taken into significant consideration. Carbon based materials have been used widely for remediating CPX from aqueous solutions. Activated carbon derived from bamboo, single layer graphene oxide, activated carbon from used lignin black liquors and hydroxylated acid treated carbon nanotubes are among the few adsorbents that were used for the removal of CPX from aqueous media (Huang et al. 2014; Li et al. 2014; Wang et al. 2015). A maximum CPX adsorption capacity of 615 mg g^{-1} was reported for bamboo based activated carbon (Wang et al., 2015).

Studies on pyrolytic biochar has gained momentum over activated carbon in the recent years due to its unique properties that are suitable for remediating a range of organic and inorganic contaminants in soil and water environments (Ahmad et al., 2014). Different feedstocks are used to produce biochar, and municipal solid waste (MSW) derived biochar has been least studied as a sorbent for antibiotic or other organic contaminants remediation (Gunarathne et al. 2018; Jayawardhana et al. 2017). The reported interactions of carbonaceous biochar with environmental organic molecules have proven its potential for binding also with antibiotic compounds (Rajapaksha et al., 2015; Vithanage et al., 2014). The versatility of biochar for remediating both organic and inorganic contaminants (Ahmad et al., 2014) can be further used to make strong active sites for CPX adsorption irrespective of the feedstock of the biochar. Although the production cost of biochar is less than activated carbon, the antibiotic adsorption capacity of biochar was limited due to two key reasons: firstly, many antibiotics like CPX are ionic nature that may cause electrostatic repulsion, and secondly ionic size of many antibiotics do not fit to the pore size of biochar (Peng et al., 2016).

Bentonite clay is a well-known adsorbent of numerous contaminants due to the high specific surface area, porosity, surface charge and cation exchange capacity (CEC) of the clay (Styszko et al. 2015). Bentonite has been proven as a potential adsorbent for tetracyclines (Li et al. 2010; Parolo et al. 2008) and oxytetracyclines (Kulshrestha et al., 2004) antibiotics. Thus, modification of biochar through structural changes or impregnation with clay materials might overcome some of the above issues and improve antibiotic removal capacity of the material (Yao et al., 2014). Clay-biochar composite materials have recently been studied for environmental remediation (Hongbo Li et al., 2017; Lin et al., 2018; Oliveira et al., 2003).

Although clay-biochar composites have been considered as potential adsorbents of several other antibiotics (Chang et al., 2016), CPX has not been considered yet. Hence, this study aims to investigate the plausibility and effectiveness of a clay-biochar composite prepared from MSW biochar and bentonite clay for CPX removal from aqueous media.

2. Experimental

2.1. Chemicals

Ciprofloxacin hydrochloride monohydrate was obtained from HIMEDIA Laboratories, India. For pH adjustments, 0.1M nitic acid and 0.1M sodium hydroxide were used. All chemicals (analytical grade) including the bentonite (86% montmorillonite, 4% silt and 10% find sand) were obtained from Sigma-Aldrich, USA.

2.2. Biochar preparation

The partially dried municipal solid waste (MSW) was collected from Gohagoda dumpsite, Kandy, Sri Lanka, and the organic fraction of the dump pile was used for producing the biochar. Pyrolysis was carried at 450 °C in a muffle furnace (Nabertherm, Germany). With a 15 °C/min increasing rate of temperature, 30 min holding time was maintained for the pyrolysis in the high temperature muffle furnace. A quick quenching was done at the end of the pyrolysis by placing the prepared char into a cold water bath to immediately activate the surface pores of the material without converting them to ash in the presence of air. For this, the pyrolyzed material was quickly transferred to a cold-water bath. Then, the material was dried in a hot air oven, and sieved through a 2 mm screen before storing it in a closed container.

2.3. Biochar-bentonite composite preparation

Bentonite (50 g) was added to 2 L of deionized water, and the suspension was sonicated for 30 min in an Ultrasonicator (Rocker-Soner 220). The MSW feedstock (250 g) was then mixed with the clay suspension, and the mixture was shaken for 2 h. The prepared slurry was oven dried at 80 °C for overnight. The MSW treated clay so prepared was converted to biochar by slow pyrolysis as described above.

2.4. Biochar and biochar-bentonite composite characterization

Powder X-ray diffraction (PXRD) patterns of the adsorbents before and after CPX adsorption were collected on a X-ray diffractometer (Rigaku, Ultima IV, Japan). Adsorbents were pressed in a glass slide sample holder, and patterns were collected using Cu Kα radiation at a wavelength of 1.54056 Å operating at 40 kV and 40 mA and scanning in the range of 2 and 65° (2θ). Scherrer equation was used for determining the mean single-crystal particle size of the clay composite adsorbent (Chen et al., 2016; Holzwarth & Gibson, 2011).

The functional groups on the adsorbent surfaces were investigated using Fourier Transform Infrared Spectroscopy. Spectra for the adsorbents before and after CPX adsorption were obtained on a Thermo Scientific, Nicolet iS10 spectrometer (USA). The spectra were obtained in transmission mode in the wavelength range of 4000- 400 cm^{-1} with a resolution of 4 cm^{-1} and 64 repetitive scans.

Field Emission Scanning Electronic Microscopy (FE-SEM) analysis was carried out to investigate the morphological features and characteristics of the adsorbents using a Hitachi SU6600 Analytical Variable Pressure FE-SEM (Japan). Adsorbent materials were mounted on an aluminum pin stub using a double-sided carbon tape, and images were collected at various resolutions.

2.5. Ciprofloxacin batch adsorption experiment

Unless otherwise stated, all adsorption experiments were carried out at 25°C under N_2 purged environment in a controlled flow just sufficient to minimize the atmospheric contamination of CO_2. At the end of each batch of experiment (after attainment of equilibration), the suspension of adsorbent was centrifuged (150 rpm) and syringe filtered (0.45 µm cellulose acetate membrane filter). The clear filtrate was then analyzed for the final concentration of CPX by UV/Vis spectrophotometer at 280 nm wavelength (Shimadzu UV160A) (Wang et al., 2010). All batch adsorption experiments were conducted with three replications, and their average results are reported here.

2.5.1. Edge experiment

The effect of pH changes on CPX adsorption by raw MSW-BC and MSW-BC-clay composite was studied by adjusting the pH of CPX solution (25 mg/L) with 0.1 M HNO_3 or NaOH in the pH range of 3.0-9.0. The adsorbent dosage was 1.0 g/L in the edge experiment. The residence time was maintained for 12 h by shaking the mixture at 150 rpm, and thereafter the final pH was measured. Samples were then centrifuged and filtered, and the filtrate was analyzed for CPX concentration as described above.

2.5.2. Kinetic experiment

In the kinetic experiment, the dosage of adsorbents was maintained at 1 g/L with 25 mg/L CPX concentration. The optimum pH (pH 7-8) for CPX adsorption (as determined in the edge experiment) and a shaking speed of 150 rpm were maintained during the kinetic experiment. The residence time was varied at 5, 15, 30 min and 2, 4, 7, 10, 15 and 24 h. After each run, samples were analyzed for CPX concentration as described above.

2.5.3. Isotherm experiment

Adsorption isotherms were determined at different CPX concentrations (10 to 250 mg/L) with a defined pH (pH 7-8), adsorbent dosage (1 g/L) and residence time (12 h). Other experimental conditions remained similar to the edge and kinetic experiments. Samples were finally analyzed for CPX concentration as described above.

2.6. Data modeling and calculation

Effective adsorption at a defined pH in the batch experiments was modeled using the pseudo second order kinetic model and Elovich equation (Supplementary Information). The isotherm experimental data were fitted to the non-linear form of the Hill model (Supplementary Information) to understand the physico-chemical mechanisms of CPX adsorption on clay-biochar composites. The Origin statistical package (version 8.0) was used to carry out the analysis of data retrieved from adsorbent characterization and adsorption experiments.

3. Results and discussion

3.1. Characterization of MSW biochar and MSW-BC-clay composite

3.1.1. PXRD Analysis

The basal spacing of the pristine bentonite was 15.49 A° (Fig. 1), which is the d_{001} reflection of pure montmorillonite with a crystal size of 17.96 nm (crystallite size calculated using Scherrer equation). The XRD pattern for biochar showed a noticeable reflection at $2\theta = 24^{O}$ which revealed the presence of quartz in the material (Zhang et al., 2015). Reflections in the patterns of bentonite and clay-biochar composite also showed traces of feldspar and dolomite (Fig. 1), which are supported by the IR spectra of these adsorbents (Fig. 2). The d_{001} reflection of montmorillonite shifted substantially to the right after formation of the clay-biochar composite, meaning the interlayer spacing of the clay mineral dropped to 12.44 Aº ($2\theta = 7.10^{o}$) in the composite as opposed to 15.49 Aº ($2\theta = 5.70^{o}$) in the raw montmorillonite. This decrease in the d-value could be attributed to the internal structural change of the clay mineral driven by the removal of water molecules during the course of synthesizing the MSW-BC-clay composite.

There was an increase in the basal spacing of montmorillonite (d_{001} reflection shifted to the left; 18.24 Aº, i.e., $2\theta = 2.42^{o}$) after treating the MSW-BC-clay composite with CPX (Fig. 1). Such an increase in d-value could be attributed to the migration of CPX molecules into the interlayer space of the clay mineral in the composite through forming H-bonds (Madusanka et al., 2015). Chang et al. (2009) observed similar behavior of montmorillonite following tetracycline adsorption by the clay mineral. Similarly, Wang et al. (2010) observed a response of the degree of swelling nature of the clay mineral (i.e., organic molecule intercalation) to the initial concentration of the organic molecules. The crystallite size in the composite decreased to 2.27 nm (as opposed to 17.96 nm of the pure montmorillonite) due to broadening of the peak and the expansion of the lattice due to the presence of amorphous biochar particles.

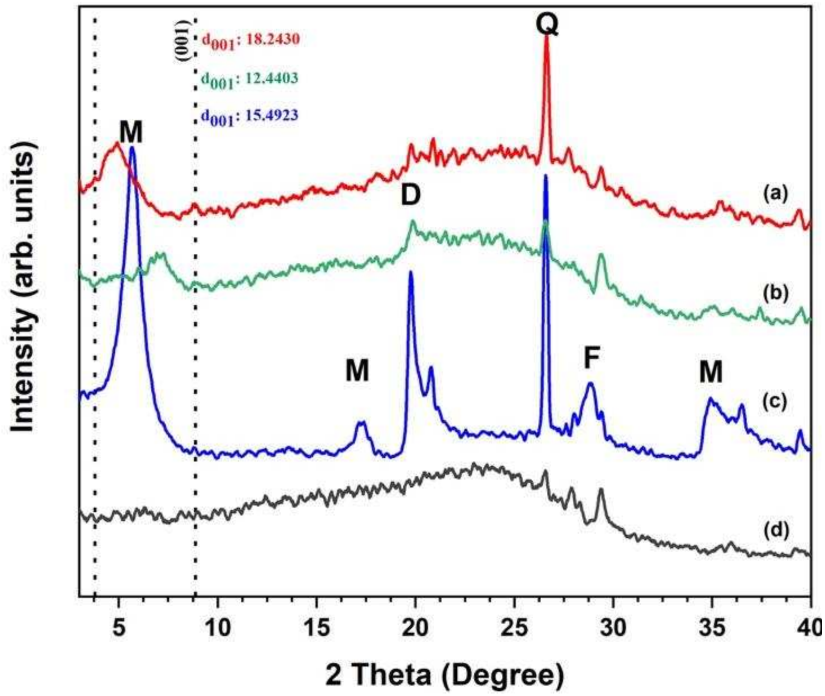

Fig. 1: PXRD patterns for (a) MSW-BC-bentonite composite with treated CPX, (b) MSW-BC-bentonite composite, (c) pristine bentonite, and (d) pristine MSW-BC, (M: montmorillonite; D-Dolomite; F-Feldspar; Q-Quartz).

3.1.2. FT-IR analysis

Transmittance spectra are shown in Fig. 2 for the pristine materials and the composites. Bands in the range of 1500-1700 cm^{-1} were attributed to the COOH stretching vibrations in the spectrum of CPX (Chen et al., 2017). Several bands observed below 1500 cm^{-1} of the CPX spectrum accounted for the effect occurred during the solvation of CPX molecules in aqueous media (Trivedi & Vasudevan, 2007). Strong band at 3630 cm^{-1} in the spectrum of bentonite indicated O-H stretching vibration, and the broadened band at around 3407 cm^{-1} implied further stretching of the water molecules (Madejová et al., 2017). Overall, these bands found in the pristine bentonite spectrum in the range of 3400-4000 cm^{-1} could be attributed to the structural hydroxyl groups of the clay associated with Si and Al (Chen et al., 2017; Fernando et al., 2012). In the spectra of the clay-biochar composite, these bands disappeared likely due to the elimination of –OH groups at high pyrolysis temperature during the synthesis of the composite. Additionally, the Si-O and Al-OH deformation bands in the bentonite spectrum appeared in the range of 1010-915 cm^{-1} in which they were stretching at 1010 cm^{-1} and bending at 913 cm^{-1}, respectively (Madusanka et al., 2017). Notably, the band at 1010 cm^{-1} in the bentonite spectrum shifted to a higher frequency (1032 cm^{-1}) in the spectrum of the clay-biochar composite likely due to a steric hindrance created during the composite synthesis (Li et al., 2017). The intensity of the 1010 cm^{-1} band drastically reduced by almost 10 fold in the composite's spectrum as compared to the pristine clay (Fig. 2). The band 1604 cm^{-1} in the bentonite spectrum appeared due to the bending vibrations of hydroxyl groups (Fig. 2) (Chen et al., 2017). This particular band showed a much broader dip in the spectra of biochar and the clay-biochar composite indicating changes in the quantity of their respective individual materials in the composite. No significant difference in the IR bands were observed in the spectra of the clay-biochar composite before and after CPX adsorption except disappearance of the CPX band at around 3600 cm^{-1} (O–H stretching).

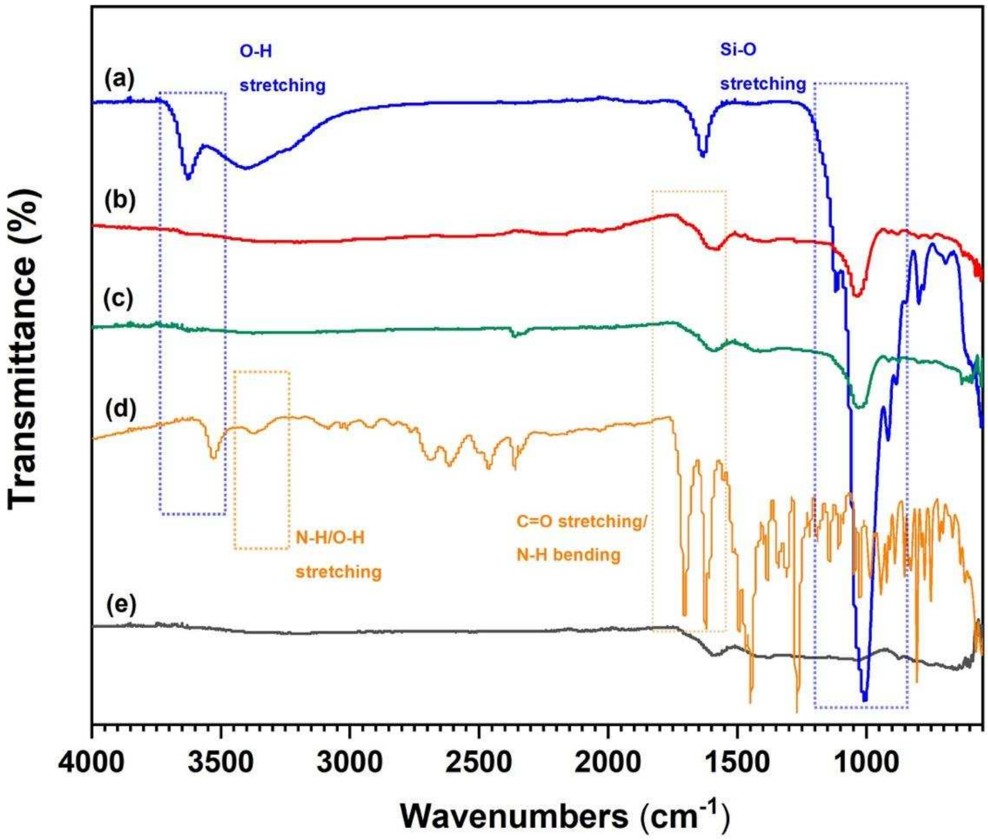

Fig. 2: FT-IR spectra of (a) pristine bentonite, (b) MSW-BC-bentonite composite with CPX, (c) biochar-bentonite composite without CPX, (d) prisitne CPX, and (e) prsitine MSW-BC

3.1.3. SEM Analysis

SEM images of the MSW-BC-clay composite at two different magnifications (x1k and x20k) are shown in Fig. 3. Since the biochar was derived from MSW, the image structures depicted here were random and disordered because of the heterogeneous nature of the biomaterials taken up for the pyrolysis. However, the presence of the bentonite clay could be confirmed through inter spatial layers or plate-like appearances that were seen at the cross- section (Fig. 3d). The irregular structures and numerous pores could be noticed in the images with the flakey clay structures embedded in the voids. The mechanisms through which interaction of the clay-biochar composite with antibiotic molecules is expected to occur are rightly embedded within the voids of these composite deciphered by the biochar impregnated with the clay. These results were supported by the PXRD and FTIR results through the increase of clay interlayer space and incorporation of new functional groups in the composite, respectively.

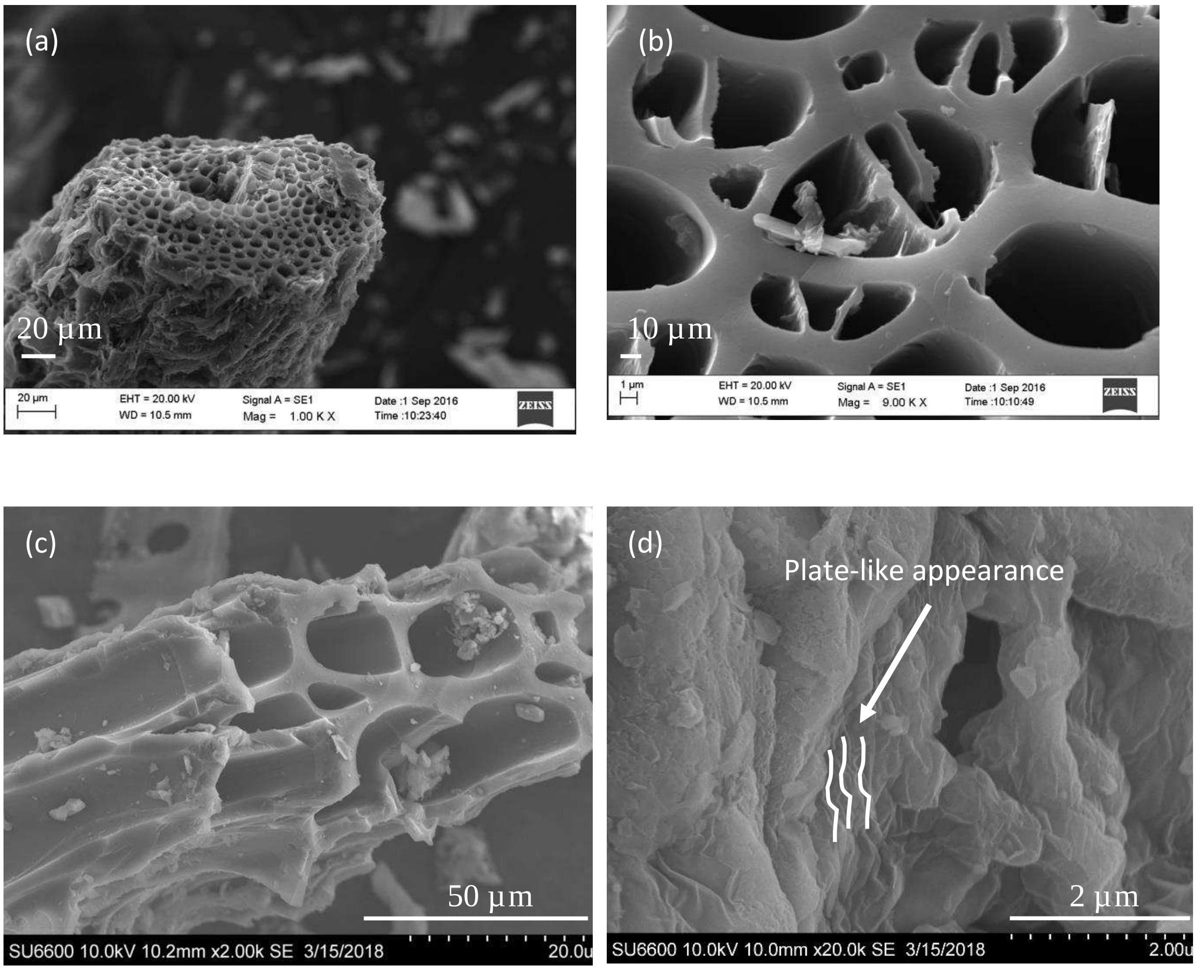

Fig. 3: SEM images of (a) MSW-BC magnification x2.00k, (b) MSW-BC magnification x40, (c) MSW-BC-bentonite composite magnification x1.00k, (d) MSW-BC-bentonite composite magnification x20.0k

3.2. Batch adsorption studies

3.2.1. Effect of initial solution pH

Preliminary batch experiments showed a limited adsorption of CPX by the untreated MSW-BC as compared with the MSW-BC-clay composite. The removal of by the CPX by MSW-

BC-clay composite could be influenced by the solution pH because both the speciation of CPX and surface charge of the adsorbent would vary according to the solution pH (Tadkaew et al., 2011).

Generally, for sulfonamide and quinolone group antibiotics, sorption capacity lowers at a minimal pH as low as pH 2 and gradually increases at an elevated pH up to pH 5 (Rajapaksha et al., 2015; Salma, Thoröe-Boveleth, Schmidt, & Tuerk, 2016). From Fig. 4, removal reaches an equilibrium at pH between 6.5-7.0, and then drops at a higher pH.

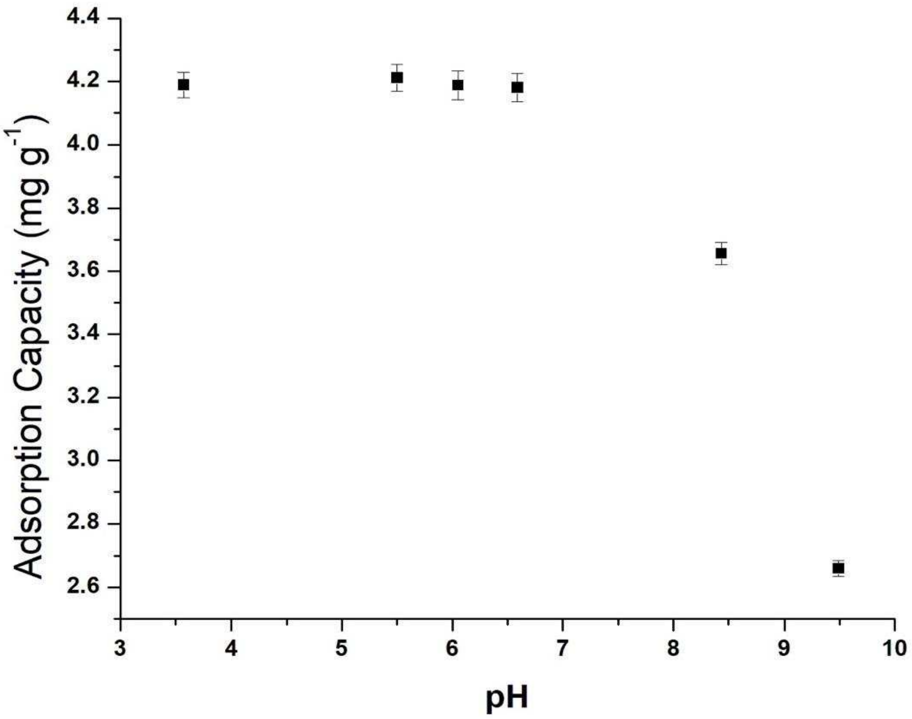

Fig. 4: Adsorption variation of CPX in bare and clay treated MSW-BC at different pHs

According to Vasudevan et al., (2009), where the behavior of the dependence of pH on the sorption of CPX onto soils was studied, proved the hypothesis on interactions that occur between the cationic amine moiety of the CPX to the negatively charged SiO_2 which pertains in the bentonite justifying the optimum edge obtained here. When the solution pH becomes in the range of 5 and 6, the active sites exists as cationic and has stronger tendency for CPX to bind (Li et al., 2018).

3.2.2. Effect of initial concentration of CPX on adsorption

The adsorption isotherm parameters along with the coefficients of determination (r^2 at $p < 0.05$) are presented in (

Table 1). Data modeling shows the best fits to Hill isotherm of CPX onto both bare and clay modified biochar (Figure 5). Values of *b* were >1 which emphasized higher interactions of CPX onto the sorbents (Gregg, 1951). Hill model is based on an assumption that the adsorption of different species onto the homogenous substrate will affect the other parts of the same substrate. This accounts for the adsorption in the first half (up to 60 mg/L) of the curve and desorption in the latter part and then adsorption (Ringot et al., 2007). The maximum adsorption capacity was achieved by composite at 286.60 mg/g which is 70 % higher than the pristine MSW-BC and thus greatly enhanced the removal with the presence of clay. This can be ascribed for the CPX molecules being intercalated between the layers of the bentonite. Hill model dictates a cooperative adsorption where on an ideal scenario, the surface active centers of the sorbents are uniformly distributed and the behavior of the sorbents and the adsorbate are steady in monolayer as in Langmuir, Hill model is a multi-layer adsorption which takes into account of the interaction between the adsorbates and adsorbents that caused the deviation from non-ideal non-Langmuir scenario (Liu, 2015; Vithanage et al., 2014). The impregnation of the clay on the biochar made a difference within the lattices of the clay to further enhance the removal efficiency of CPX.

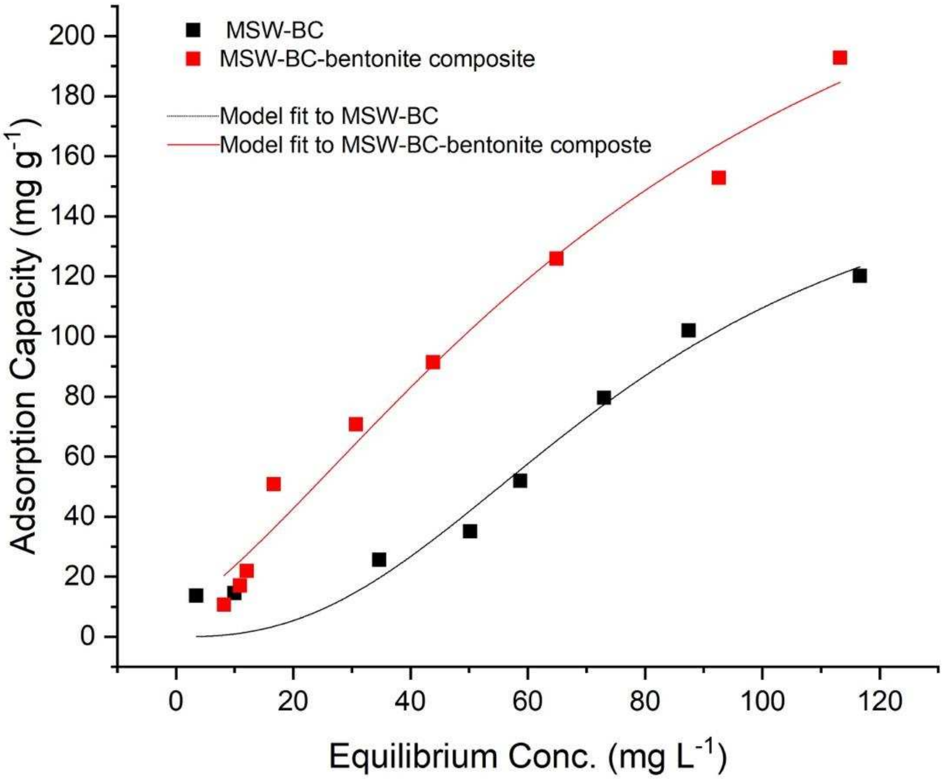

Figure 5: Hill isotherm model fit for pristine MSW-BC and MSW-BC-clay composite

Table 1: Hill isotherm parameters for CPX adsorption

Adsorbent	**q_{max} (mg g^{-1})**	**b (L mg^{-1})**	**K_h**	**r^2**
MSW-BC	167.610	2.507	0.013	0.955
MSW- BC-clay composite	286.604	1.653	0.032	0.981

3.2.3. Effect of contact time on adsorption

Adsorption of CPX variation with time shows a subsequent increase and then stays at plateau finally reaching equilibrium with time (Fig. 6). The decrease in the active sites as the time progresses is results a decrease in the adsorption rate. A rapid adsorption was observed within 60 minutes of the residence time of CPX with the biochar resulting in an adsorption of 22.4 mg/g until the rate reaches an equilibrium. A similar trend is observed for the MSW-BC-clay composite. Elovich model fitted the kinetic data indicating that the composite has a high surface activity for the cationic part of the CPX molecule that ionizes at different pH (Chen et al., 2017). Table 2 shows the kinetic model parameters and coefficients of determination (r^2 at $p < 0.05$) for CPX adsorption onto MSW-BC and MSW-BC-clay composite. Elovich best fit for the composite also indicates a more dominative chemisorption mechanism as in chemical bonds between the different ionization moiety of the CPX molecule and the sorbents that is with a heterogenous surface (Inyang et al., 2015). Since, bentonite is a mixture of minerals including montmorillonite, the available cations in the interlayer of the bentonite get replaced with the cationic NH_2^+ of the CPX molecules, and the negative ends of the MSW-BC may bind with these cations forming ion pairs (for instance, Na^+, Ca^{2+} in the case of montmorillonite) (Chen et al., 2016).

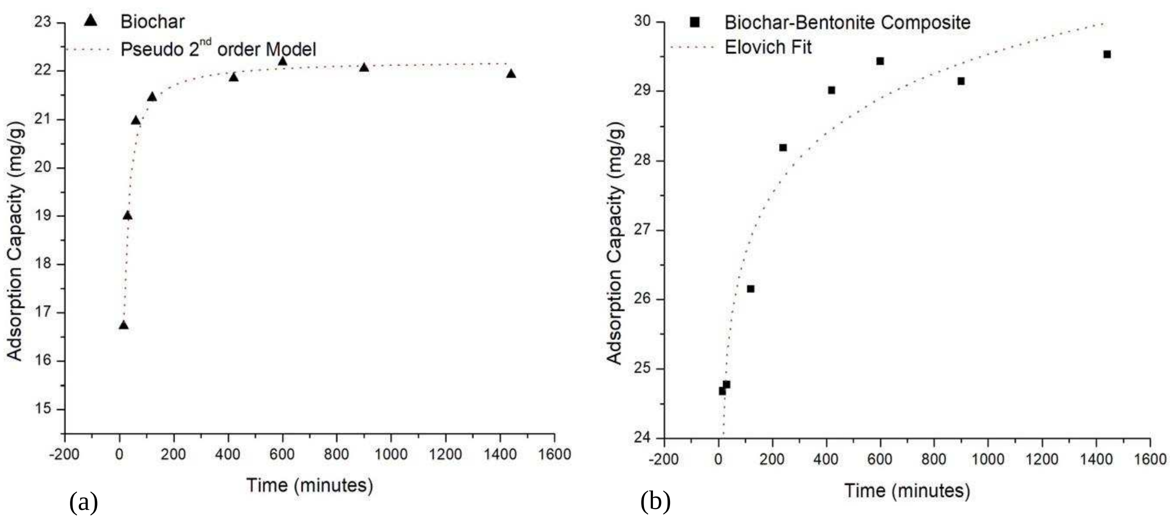

(a) (b)

Fig. 6: (a) Pseudo-second order kinetic fit for pristine MSW-BC, and (b) Elovich fit for MSW-BC-clay composite

Table 2: Kinetic model parameters and coefficients of determination of adsorption of CPX on to biochar and biochar-bentonite composite

Model	**Parameters for MSW-BC**	
Pseudo-second-order	k_2 (g mg^{-1} min^{-1})	0.009
	q_e (mg g^{-1})	22.227
	r^2	0.989
Model	**Parameters for MSW-BC-clay composite**	

Elovich	a (g mg^{-1} min^{-1})	$2.64x10^7$
	b (g mg^{-1} min^{-1})	0.805
	r^2	0.937

3.3. Adsorption mechanisms

According to FTIR analysis, there is an underlying difference between the pristine MSW-BC and the composites prepared where the disappearance of O-H group is accountable for the clay modification made as well as the deduced intensity of the SiO_2 absorption bands. This can be further confirmed through the peaks obtained from the PXRD intensity at 2θ of 24^O which decreased with the introduction of the MSW-BC. Adsorption in clays for most cases occurs in four different pathways: at the surface itself, on the edges of the plates and the interlayer spaces between two consecutive layers (Chen et al., 2016). Ideally, in clay the dominant cation is saturated with two layers of water molecules (Wang et al., 2010), however, there is a dehydration involved when the CPX is being introduced into the lattice. This attributes to the broadening of the peaks in PXRD where the adsorbed CPX are distributed in the lattice in a disordered manner. The electrostatic interactions between the different functional groups of the MMT and the BC of the sorbents competing with the other functional groups of the CPX molecule make it a stronger adsorption. The cationic dominant group in the clay involves for the coulombic attraction with the amide group of the CPX according to Vasudevan et al. (2009). This explains the heterogeneity deduced from the kinetic modeling of the MSW-BC-bentonite composite due to the competing ions in the same CPX molecule with different active sites of the sorbents. Chen and Zhou (2008) suggested that the sorption of organic contaminants onto biochar is due to two kinds of interactions: adsorption on the carbonized fraction of the biochar and the partition in the noncarbonized fractions of the biochar.

The possible chemical equations for the CPX adsorption reaction can be postulated as follows:

At acidic conditions:

$$H^+ + \boldsymbol{R} - NH \ \rightarrow \boldsymbol{R} - NH_2^+$$

$$\boldsymbol{R} - NH_2^+ + \boldsymbol{M}^- \ \rightarrow \boldsymbol{R} - NH_2\boldsymbol{M}$$

At alkaline conditions:

$$\boldsymbol{R} - COO^- + Na^+ \ \rightarrow \ \boldsymbol{R} - COONa$$

Where, $\boldsymbol{R}$ is the group accounting from CPX, and $\boldsymbol{M}$ is the group arising from the bentonite.

This explains the simultaneous exchange of ions between the sorbents and the CPX where interactions are stronger, for instance, hydrogen-bonding induced adsorption between the oxygen-containing functional group of the CPX with free hydroxyl group on the MSW-BC clay composite (Sun et al., 2011; Zhang et al., 2015). Through the modification done on the MSW-BC with bentonite, more active sites may have generated and functional groups have been modified for a stronger ionic electrostatic attraction for CPX in aqueous solution.

4. Conclusions

Municipal solid waste was engineered successfully to prepare clay-BC composite. The MSW-BC exhibited better affinity for the CPX removal than the pristine MSW-BC. Interlayer encapsulation of CPX into the clay-BC composite was supported from both PXRD and FTIR results. Sorption of CPX was pH-dependent demonstrating a high removal at a mild acidic condition. The modification of MSW-BC with clay greatly enhanced the active sites where the different functional groups cling on the composite more efficiently than the pristine clay or MSW-BC. The MSW-BC-clay and CPX interactions should be further studied and directed towards taking the ionization effect of the CPX molecule in different solution conditions into account, to further immobilize CPX onto the sorbent for the efficient removal.

Acknowledgements

Financial support from the grant ASP/01/RE/SCI/2017/83 from the Research Council, and the analytical support from the Instrument Center, Faculty of Applied Sciences, University of Sri Jayewardenepura are acknowledged.

References

Ahmad, M., Rajapaksha, A. U., Lim, J. E., Zhang, M., Bolan, N., Mohan, D., … Ok, Y. S. (2014). Biochar as a sorbent for contaminant management in soil and water: A review. Chemosphere. https://doi.org/10.1016/j.chemosphere.2013.10.071

Amorim, C. L., Moreira, I. S., Maia, A. S., Tiritan, M. E., & Castro, P. M. L. (2014). Biodegradation of ofloxacin, norfloxacin, and ciprofloxacin as single and mixed substrates by Labrys portucalensis F11. Applied Microbiology and Biotechnology, 98(7), 3181–3190. https://doi.org/10.1007/s00253-013-5333-8

Azanu, D., Styrishave, B., Darko, G., Weisser, J. J., & Abaidoo, R. C. (2018). Occurrence and risk assessment of antibiotics in water and lettuce in Ghana. Science of the Total Environment, 622–623, 293–305. https://doi.org/10.1016/j.scitotenv.2017.11.287

Chang, P. H., Jiang, W. T., Li, Z., Kuo, C. Y., Wu, Q., Jean, J. S., & Lv, G. (2016). Interaction of ciprofloxacin and probe compounds with palygorskite PFl-1. Journal of Hazardous Materials, 303, 55–63. https://doi.org/10.1016/j.jhazmat.2015.10.012

Chang, P. H., Li, Z., Jiang, W. T., & Jean, J. S. (2009). Adsorption and intercalation of tetracycline by swelling clay minerals. Applied Clay Science, 46(1), 27–36. https://doi.org/10.1016/j.clay.2009.07.002

Chen, B., & Zhou, D. (2008). Transitional Adsorption and Partition of Nonpolar and Polar

Aromatic Contaminants by Biochars of Pine Needles with Different Pyrolytic Temperatures. Environmental Science & Technology, 42(14), 5137–5143.
Chen, L., Chen, X. L., Zhou, C. H., Yang, H. M., Ji, S. F., Tong, D. S., … Chu, M. Q. (2017). Environmental-friendly montmorillonite-biochar composites: Facile production and tunable adsorption-release of ammonium and phosphate. Journal of Cleaner Production, 156, 648–659. https://doi.org/10.1016/j.jclepro.2017.04.050
Chen, L., Zhou, C. H., Fiore, S., Tong, D. S., Zhang, H., Li, C. S., … Yu, W. H. (2016). Functional magnetic nanoparticle/clay mineral nanocomposites: Preparation, magnetism and versatile applications. Applied Clay Science, 127–128(June), 143–163. https://doi.org/10.1016/j.clay.2016.04.009
Espinosa, K., Park, J. A., Gerrity, J. J., Buono, S., Shearer, A., Dick, C., … Hess, D. (2015). Fluoroquinolone resistance in neisseria gonorrhoeae after cessation of ciprofloxacin usage in San Francisco: Using molecular typing to investigate strain turnover. Sexually Transmitted Diseases, 42(2), 57–63. https://doi.org/10.1097/OLQ.0000000000000233
Fernando, S., Madusanka, N., & Kottegoda, N. (2012). Zinc Oxide Nanoparticles as an Activator for Natural Rubber Latex. Nadeeshadassooriya.Com, (3). Retrieved from http://nadeeshadassooriya.com/docs/ZnO nano.pdf
Gregg, S. J. (1951). The Surface Chemistry of Solids. Oxford university press.
Gunarathne, V., Ashiq, A., & Ginige, M. P. (2018). Green Adsorbents for Pollutant Removal, 19. https://doi.org/10.1007/978-3-319-92162-4
Holzwarth, U., & Gibson, N. (2011). The Scherrer equation versus the ‘ Debye – Scherrer equation .’ Nature Nanotechnology, 6(9), 534. https://doi.org/10.1038/nnano.2011.145
Huang, L., Wang, M., Shi, C., Huang, J., & Zhang, B. (2014). Adsorption of tetracycline and ciprofloxacin on activated carbon prepared from lignin with H3PO4activation. Desalination and Water Treatment, 52(13–15), 2678–2687. https://doi.org/10.1080/19443994.2013.833873
Huang, X., Zheng, J., Liu, C., Liu, L., Liu, Y., & Fan, H. (2017). Removal of antibiotics and resistance genes from swine wastewater using vertical flow constructed wetlands: Effect of hydraulic flow direction and substrate type. Chemical Engineering Journal, 308, 692–699. https://doi.org/10.1016/j.cej.2016.09.110
Inyang, M., Gao, B., Zimmerman, A., Zhou, Y., & Cao, X. (2015). Sorption and cosorption of lead and sulfapyridine on carbon nanotube-modified biochars. Environmental Science and Pollution Research, 22(3), 1868–1876. https://doi.org/10.1007/s11356-014-2740-z
Jayawardhana, Y., Mayakaduwa, S. S., Kumarathilaka, P., Gamage, S., & Vithanage, M. (2017). Municipal solid waste-derived biochar for the removal of benzene from landfill leachate. Environmental Geochemistry and Health, 1–15. https://doi.org/10.1007/s10653-017-9973-y
Kanakaraju, D., Glass, B. D., & Oelgemöller, M. (2018). Advanced oxidation process-mediated removal of pharmaceuticals from water: A review. Journal of Environmental Management, 219, 189–207. https://doi.org/10.1016/j.jenvman.2018.04.103
Kim, K. S., Kam, S. K., & Mok, Y. S. (2015). Elucidation of the degradation pathways of sulfonamide antibiotics in a dielectric barrier discharge plasma system. Chemical Engineering Journal, 271, 31–42. https://doi.org/10.1016/j.cej.2015.02.073
Kulshrestha, P., Giese, R. F., & Aga, D. S. (2004). Investigating the molecular interactions of oxytetracycline in clay and organic matter: Insights on factors affecting its mobility in soil. Environmental Science and Technology, 38(15), 4097–4105. https://doi.org/10.1021/es034856q
Larsson, D. G. J., de Pedro, C., & Paxeus, N. (2007). Effluent from drug manufactures contains extremely high levels of pharmaceuticals. Journal of Hazardous Materials, 148(3), 751–755. https://doi.org/10.1016/j.jhazmat.2007.07.008

Li, B., & Zhang, T. (2010). Biodegradation and adsorption of antibiotics in the activated sludge process. Environmental Science and Technology, 44(9), 3468–3473. https://doi.org/10.1021/es903490h

Li, H., Dong, X., da Silva, E. B., de Oliveira, L. M., Chen, Y., & Ma, L. Q. (2017). Mechanisms of metal sorption by biochars: Biochar characteristics and modifications. Chemosphere, 178, 466–478. https://doi.org/10.1016/j.chemosphere.2017.03.072

Li, H., Zhang, D., Han, X., & Xing, B. (2014). Adsorption of antibiotic ciprofloxacin on carbon nanotubes: PH dependence and thermodynamics. Chemosphere, 95, 150–155. https://doi.org/10.1016/j.chemosphere.2013.08.053

Li, J., Yu, G., Pan, L., Li, C., You, F., Xie, S., … Shang, X. (2018). Study of ciprofloxacin removal by biochar obtained from used tea leaves. Journal of Environmental Sciences (China), 1–11. https://doi.org/10.1016/j.jes.2017.12.024

Li, M., Wei, D., & Du, Y. (2014). Acute toxicity evaluation for quinolone antibiotics and their chlorination disinfection processes. Journal of Environmental Sciences (China), 26(9), 1837–1842. https://doi.org/10.1016/j.jes.2014.06.023

Li, Y., Wang, Z., Xie, X., Zhu, J., Li, R., & Qin, T. (2017). Removal of Norfloxacin from aqueous solution by clay-biochar composite prepared from potato stem and natural attapulgite. Colloids and Surfaces A: Physicochemical and Engineering Aspects, 514, 126–136. https://doi.org/10.1016/j.colsurfa.2016.11.064

Li, Z., Chang, P. H., Jean, J. S., Jiang, W. T., & Wang, C. J. (2010). Interaction between tetracycline and smectite in aqueous solution. Journal of Colloid and Interface Science, 341(2), 311–319. https://doi.org/10.1016/j.jcis.2009.09.054

Liao, X., Li, B., Zou, R., Dai, Y., Xie, S., & Yuan, B. (2016). Biodegradation of antibiotic ciprofloxacin: pathways, influential factors, and bacterial community structure. Environmental Science and Pollution Research, 23(8), 7911–7918. https://doi.org/10.1007/s11356-016-6054-1

Lin, J., Jiang, B., & Zhan, Y. (2018). Effect of pre-treatment of bentonite with sodium and calcium ions on phosphate adsorption onto zirconium-modified bentonite. Journal of Environmental Management, 217, 183–195. https://doi.org/10.1016/j.jenvman.2018.03.079

Liu, S. (2015). Cooperative adsorption on solid surfaces. Journal of Colloid and Interface Science, 450, 224–238. https://doi.org/10.1016/j.jcis.2015.03.013

Madejová, J., Gates, W. P., & Petit, S. (2017). IR Spectra of Clay Minerals. Developments in Clay Science (Vol. 8). https://doi.org/10.1016/B978-0-08-100355-8.00005-9

Madusanka, N., De Silva, K. M. N., & Amaratunga, G. (2015). A curcumin activated carboxymethyl cellulose-montmorillonite clay nanocomposite having enhanced curcumin release in aqueous media. Carbohydrate Polymers, 134, 695–699. https://doi.org/10.1016/j.carbpol.2015.08.030

Madusanka, N., Shivareddy, S. G., Eddleston, M. D., Hiralal, P., Oliver, R. A., & Amaratunga, G. A. J. (2017). Dielectric behaviour of montmorillonite/cyanoethylated cellulose nanocomposites. Carbohydrate Polymers, 172, 315–321. https://doi.org/10.1016/j.carbpol.2017.05.057

Martinez-Carballo, E., Gonzalez-Barreiro, C., Scharf, S., & Gans, O. (2007). Environmental monitoring study of selected veterinary antibiotics in animal manure and soils in Austria. Environ Pollut, 148(2), 570–579. https://doi.org/10.1016/j.envpol.2006.11.035

Maul, J. D., Schuler, L. J., Belden, J. B., Whiles, M. R., & Lydy, M. J. (2006). Effects of the anibiotic ciprofloxacin on stream microbial communities and detrivorous macroinvertebrates. Environmental Toxicology and Chemistry, 25(6), 1598–1606.

Nowara, A., Burhenne, J., & Spiteller, M. (1997). Binding of flouroquinolone carboxylic acid derivatives to clay minerals. J Agric Food Chem, 45(4), 1459–1463.

Oberlé, K., Capdeville, M. J., Berthe, T., Budzinski, H., & Petit, F. (2012). Evidence for a complex relationship between antibiotics and antibiotic-resistant escherichia coli: From medical center patients to a receiving environment. Environmental Science and Technology, 46(3), 1859–1868. https://doi.org/10.1021/es203399h

Oliveira, L. C. A., Rios, R. V. R. A., Fabris, J. D., Sapag, K., Garg, V. K., & Lago, R. M. (2003). Clay-iron oxide magnetic composites for the adsorption of contaminants in water. Applied Clay Science, 22(4), 169–177. https://doi.org/10.1016/S0169-1317(02)00156-4

Parolo, M. E., Savini, M. C., Vallés, J. M., Baschini, M. T., & Avena, M. J. (2008). Tetracycline adsorption on montmorillonite: pH and ionic strength effects. Applied Clay Science, 40(1–4), 179–186. https://doi.org/10.1016/j.clay.2007.08.003

Patrolecco, L., Rauseo, J., Ademollo, N., Grenni, P., Cardoni, M., Levantesi, C., … Caracciolo, A. B. (2018). Persistence of the antibiotic sulfamethoxazole in river water alone or in the co-presence of ciprofloxacin. Science of the Total Environment, 640–641, 1438–1446. https://doi.org/10.1016/j.scitotenv.2018.06.025

Peng, B., Chen, L., Que, C., Yang, K., Deng, F., Deng, X., … Wu, M. (2016). Adsorption of Antibiotics on Graphene and Biochar in Aqueous Solutions Induced by π-π Interactions. Scientific Reports, 6(1), 31920. https://doi.org/10.1038/srep31920

Philip, J. M., Aravind, U. K., & Aravindakumar, C. T. (2018). Emerging contaminants in Indian environmental matrices – A review. Chemosphere, 190, 307–326. https://doi.org/10.1016/j.chemosphere.2017.09.120

Rajapaksha, A. U., Vithanage, M., Ahmad, M., Seo, D. C., Cho, J. S., Lee, S. E., … Ok, Y. S. (2015). Enhanced sulfamethazine removal by steam-activated invasive plant-derived biochar. Journal of Hazardous Materials, 290, 43–50. https://doi.org/10.1016/j.jhazmat.2015.02.046

Ringot, D., Lerzy, B., Chaplain, K., Bonhoure, J. P., Auclair, E., & Larondelle, Y. (2007). In vitro biosorption of ochratoxin A on the yeast industry by-products: Comparison of isotherm models. Bioresource Technology, 98(9), 1812–1821. https://doi.org/10.1016/j.biortech.2006.06.015

Salma, A., Thoröe-Boveleth, S., Schmidt, T. C., & Tuerk, J. (2016). Dependence of transformation product formation on pH during photolytic and photocatalytic degradation of ciprofloxacin. Journal of Hazardous Materials, 313, 49–59. https://doi.org/10.1016/j.jhazmat.2016.03.010

Sanderson, H., Fricker, C., Brown, R. S., Majury, A., & Liss, S. N. (2016). Antibiotic resistance genes as an emerging environmental contaminant. Environmental Reviews, 24(2), 205–218. https://doi.org/10.1139/er-2015-0069

Sarmah, A. K., Meyer, M. T., & Boxall, A. B. A. (2006). A global perspective on the use,sales,exposure pathways ,occurrence,fate and effects of veterinary antibiotics(VAs) in the environment. Chemosphere, 65(5), 725–759. https://doi.org/10.1016/j.chemosphere.2006.03.026

Styszko, K., Nosek, K., Motak, M., & Bester, K. (2015). Preliminary selection of clay minerals for the removal of pharmaceuticals, bisphenol A and triclosan in acidic and neutral aqueous solutions. Comptes Rendus Chimie, 18(10), 1134–1142. https://doi.org/10.1016/j.crci.2015.05.015

Sun, K., Keiluweit, M., Kleber, M., Pan, Z., & Xing, B. (2011). Sorption of fluorinated herbicides to plant biomass-derived biochars as a function of molecular structure. Bioresource Technology, 102(21), 9897–9903. https://doi.org/10.1016/j.biortech.2011.08.036

Tadkaew, N., Hai, F. I., McDonald, J. A., Khan, S. J., & Nghiem, L. D. (2011). Removal of trace organics by MBR treatment: The role of molecular properties. Water Research,

45(8), 2439–2451. https://doi.org/10.1016/j.watres.2011.01.023
Trivedi, P., & Vasudevan, D. (2007). Spectroscopic investigation of ciprofloxacin speciation at the goethite-water interface. Environmental Science and Technology, 41(9), 3153–3158. https://doi.org/10.1021/es061921y
Vasudevan, D., Bruland, G. L., Torrance, B. S., Upchurch, V. G., & MacKay, A. A. (2009). pH-dependent ciprofloxacin sorption to soils: Interaction mechanisms and soil factors influencing sorption. Geoderma, 151(3–4), 68–76. https://doi.org/10.1016/j.geoderma.2009.03.007
Vithanage, M., Rajapaksha, A. U., Tang, X., Thiele-Bruhn, S., Kim, K. H., Lee, S. E., & Ok, Y. S. (2014). Sorption and transport of sulfamethazine in agricultural soils amended with invasive-plant-derived biochar. Journal of Environmental Management, 141, 95–103. https://doi.org/10.1016/j.jenvman.2014.02.030
Wang, C. J., Li, Z., Jiang, W. T., Jean, J. S., & Liu, C. C. (2010). Cation exchange interaction between antibiotic ciprofloxacin and montmorillonite. Journal of Hazardous Materials, 183(1–3), 309–314. https://doi.org/10.1016/j.jhazmat.2010.07.025
Wang, Y. X., Ngo, H. H., & Guo, W. S. (2015). Preparation of a speci fi c bamboo based activated carbon and its application for cipro fl oxacin removal Total-V. Science of the Total Environment, 533(2015), 32–39. https://doi.org/10.1016/j.scitotenv.2015.06.087
Yao, Y., Gao, B., Fang, J., Zhang, M., Chen, H., Zhou, Y., … Yang, L. (2014). Characterization and environmental applications of clay-biochar composites. Chemical Engineering Journal, 242, 136–143. https://doi.org/10.1016/j.cej.2013.12.062
Yi, K., Wang, D., QiYang, Li, X., Chen, H., Sun, J., … Zeng, G. (2017). Effect of ciprofloxacin on biological nitrogen and phosphorus removal from wastewater. Science of the Total Environment, 605–606, 368–375. https://doi.org/10.1016/j.scitotenv.2017.06.215
Yu, F., Li, Y., Han, S., & Ma, J. (2016). Adsorptive removal of antibiotics from aqueous solution using carbon materials. Chemosphere, 153, 365–385. https://doi.org/10.1016/j.chemosphere.2016.03.083
Zhang, J., Lü, F., Zhang, H., Shao, L., Chen, D., & He, P. (2015). Multiscale visualization of the structural and characteristic changes of sewage sludge biochar oriented towards potential agronomic and environmental implication. Scientific Reports, 5(1), 9406. https://doi.org/10.1038/srep09406
Zhang, X., McGrouther, K., He, L., Huang, H., Lu, K., & Wang, H. (2015). Biochar for organic Contaminant Management in Soil. Biochar: Production, Characterization and Applications, 140–165.
Zhao, L., Dong, Y. H., & Wang, H. (2010). Residues of veterinary antibiotics in manures from feedlot livestock in eight provinces of China. Science of the Total Environment, 408(5), 1069–1075. https://doi.org/10.1016/j.scitotenv.2009.11.014

Supplementary Data

Municipal solid waste biochar-bentonite composite for the removal of antibiotic ciprofloxacin from aqueous media

Ahmed Ashiq[1], Nadeesh M. Adassooriya[1], Binoy Sarkar[2,3*], Anushka Upamali Rajapaksha[1], Yong Sik Ok[4], Meththika Vithanage[1, 5*]

[1] Ecosphere Resilience Research Centre, Faculty of Applied Science, University of Sri Jayewardenepura, Sri Lanka

[2] Department of Animal and Plant Sciences, The University of Sheffield, Sheffield, S10 2TN, United Kingdom

[3] Future Industries Institute, University of South Australia, Mawson Lakes, SA 5095, Australia

[4] Korea Biochar Research Center, O-Jeong Eco-Resilience Institute (OJERI) & Division of Environmental Science and Ecological Engineering, Korea University, Seoul 02841, South Korea

[5] Molecular Microbiology and Human Diseases, National Institute of Fundamental Studies, Kandy 20000, Sri Lanka

*Co-corresponding authors:

Dr Binoy Sarkar; The University of Sheffield; E-mail: b.sarkar@sheffield.ac.uk; and

Dr Meththika Vithanage; University of Sri Jayewardenepura; E-mail: meththika@sjp.ac.lk

Supplementary Data Summary:

- Number of pages: 3
- Appendix: Experimental and Data calculations
- Number of figure: 1

Appendix:

Experimental

A brief methodology is as shown below (Fig. S1).

Figure S7: Brief pictorial of methods followed for biochar-bentonite composite preparation

Experimental Data Modeling and Calculations

The amount of CPX adsorbed on the biochar adsorbents and the antibiotic adsorption capacity (q_e) were determined using the equation below:

$$\%\ Removal = \frac{C_i - C_f}{C_i} \times 100$$

$$Adsorption\ capacity\ q_e \left(\frac{mg}{g}\right) = \frac{C_i - C_f}{M_s} \times V$$

Where, V is the volume of the solution (L), M_s is the weight of adsorbent (g), C_i is the initial concentration (mg.L^{-1}) and C_f is the final concentration (mg.L^{-1}).

To investigate the mechanism of adsorption of CPX onto the biochar based adsorbents, adsorption kinetic experiments were conducted for both the pristine biochar and the composite. The adsorption kinetic data were fitted to pseudo second order kinetic model and Elovich equation.

The pseudo second order kinetic equation can be expressed as (Ho and McKay 1999):

$$q = \frac{K_2 q_e^2 t}{1 + K_2 q_e t}$$

Where, q_e is the sorption capacity at equilibrium (mg.g^{-1}), K_2 rate constant of the pseudo second-order sorption (g.mg^{-1}.min^{-1}) and t is the time in minutes.

The Elovich equation can be written as (Chien and Clayton 1980):

$$q = \frac{1}{b}\ln(ab) + \frac{1}{b}\ln(t)$$

Where, a is the initial sorption rate (g.mg^{-1}.min^{-1}), and b is the adsorption constant (g.mg^{-1}.min^{-1}).

The reaction or diffusion pathway that occurs on the sorbent represents the kinetics involved in the batches performed.

The isotherm experimental data were made to fit using a non-linear model, viz., Hill model, to provide for the best fit of the physico-chemical mechanisms for adsorption. The Hill isotherm equation is described as:

$$q_{ads} = \frac{q_m(KC_e)^b}{1 + (KC_e)^b}$$

Where, K is the Hill constant and b is the empirical parameter variable with changing heterogenous environment (Foo and Hameed 2010). The parameter b should be greater than 1 for a positive interaction (Weerasooriya et al. 2006).

References

Chien, S. H., and W. R. Clayton. 1980. “Application of Elovich Equation to the Kinetics of Phosphate Release and Sorption in Soils1.” Soil Science Society of America Journal 44(2): 265. https://www.soils.org/publications/sssaj/abstracts/44/2/SS0440020265.

Foo, K.Y., and B.H. Hameed. 2010. “Insights into the Modeling of Adsorption Isotherm Systems.” Chemical Engineering Journal 156(1): 2–10. http://linkinghub.elsevier.com/retrieve/pii/S1385894709006147.

Ho, Y S, and G McKay. 1999. “Pseudo-Second Order Model for Sorption Processes.” Process Biochemistry 34(5): 451–65. http://www.sciencedirect.com/science/article/pii/S0032959298001125.

Weerasooriya, Rohan, Wasana Seneviratne, Heasha A Kathriarachchi, and Heinz J Tobschall. 2006. “Thermodynamic Assessment of Hg (II)–Gibbsite Interactions.” Journal of colloid and interface science 301(2): 452–60.